Results in Physics 9 (2018) 1371–1376

Contents lists available at ScienceDirect

Results in Physics

journal homepage: www.elsevier.com/locate/rinp

Optical properties of zinc lead tellurite glasses

Salah Hassan Alazoumi[a,e,*], Sidek Abdul Aziz[a,b,*], R. El-Mallawany[c], Umar Sa'ad Aliyu[d], Halimah Mohamed Kamari[a,b], Mohd Hafiz Mohd Mohd Zaid[a,b], Khamirul Amin Matori[a,b], Abdulbaset Ushah[a]

[a] Department of Physics, Faculty of Science, Universiti Putra Malaysia, 43400 UPM Serdang, Selangor, Malaysia
[b] Materials Synthesis and Characterization Laboratory, Institute of Advanced Technology, Universiti Putra Malaysia, 43400 UPM Serdang, Selangor, Malaysia
[c] Physics Department, Faculty of Science, Menoufia University, Egypt
[d] Department of Physics, Faculty of Science, Federal University Lafia, Nigeria
[e] Physics Department, Faculty of Science, Gharyan University, Libya

ARTICLE INFO

Keywords:
Tellurite
Glass
Optical band gap
Refractive index

ABSTRACT

Tellurite glass systems in the form of $[ZnO]_x$ $[(TeO_2)_{0.7}$-$(PbO)_{0.3}]_{1-x}$ with x = 0.15, 0.17, 0.20, 0.22 and 0.25 mol % were prepared using the melt quenching technique. XRD of the prepared samples have been measured for all samples. Both FTIR (280–4000 cm^{-1}) and UV-Vis (200–800 nm) spectra have been measured. Optical band gap and refractive index were calculated for every glass sample. Density of glass, molar volume and oxygen packing density (OPD) were obtained. Values of the direct, indirect band gap ranged were found in the range 3.41–3.94 eV and 2.40–2.63 eV with increasing of ZnO concentration. Refractive index 2.58 and dielectric constant 6.66 were heigh at 17 ZnO mol% concentration. Molar polarizability, metallization criterion, polaron radius have been calculated for every glass composition.

Introduction

Glasses based on tellurium dioxide and modified by heavy metal oxides have properties promising for various optical applications. Many different works have been carried out in the study of the physical properties of different composition of tellurite glasses [1–5]. Due to their versatility in terms applications, tellurite glasses have received some scientific and technological attentions in the recent years [6,7,8]. The glasses have shown great promise in optical fiber technology, lasers, sensors, optical fibers, solar cells [9], memory switching devices, optoelectronic, gas sensors, and optical waveguides applications [10,11]. The glasses have been so important in the photonic technology and other applications because of their excellence in terms of high index of refraction, dielectric constant, wide spectral region transparency, resistance to corrosion, chemical and thermal stability and low melting point [8,9].

The present work presents a study on the effect of ZnO on density, the oxygen parking density (O.P.D), FTIR spectra, optical band gap, Urbach energy, reflection loss, molar refractive index, optical transmission coefficient, molar polarizability and dielectric constant for tellurite glass systems in the form of $[ZnO]_x$ $[(TeO_2)_{0.7}$-$(PbO)_{0.3}]_{1-x}$ with x = 0.15, 0.17, 0.20, 0.22 and 0.25 mol%.

Experimental work

$[ZnO]_x$ $[(TeO_2)_{0.7}$-$(PbO)_{0.3}]_{1-x}$ glass system was prepared by mixing specific weights of high purity oxides, tellurium oxide, TeO_2 (Alfa Aesar, 99.99%), lead oxide, PbO (Alfa Aesar, 99.99%) and zinc oxide, ZnO (Alfa Aesar, 99.99%). The homogenization of the 15 g of chemicals mixtures was effected by repeated grinding using a mortar for 30 min. The mixtures were preheated in a crucible (alumina) at 280 °C for one hour in the electric furnace; the crucible was then transferred to the another electrical furnace for one hour at a temperature 850–900 °C. The mixture melt then turned into a stainless steel cylindrical shaped split stainless steel mould that has been preheated. After the process of quenching, the solid sample of glass was annealed at 280 °C for an hour to avoid the mechanical strain developed during the process of quenching and then left to cool down to ambient temperature. The glass samples were cut into about 2 mm thickness using the low-speed diamond blade to make great parallel surfaces for UV-Vis charaterization. Both surfaces of the samples were polished using a polishing machine with sandpaper to achieve a plane parallelism, and a part of the sample cut was grinded into a powdered from for XRD and FTIR characterizations.

Density measurement of the glass samples was carried out at room temperature using a densitometer model (MD-300SDensimeter)

* Corresponding authors at: Department of Physics, Faculty of Science, Universiti Putra Malaysia, 43400 UPM Serdang, Selangor, Malaysia.
E-mail addresses: selazomi@gmail.com (S.H. Alazoumi), sidek@upm.edu.my (S.A. Aziz).

https://doi.org/10.1016/j.rinp.2018.04.041
Received 10 March 2018; Received in revised form 12 April 2018; Accepted 13 April 2018
Available online 27 April 2018

employing the principle of Archimedes with distilled water used as the fluid of immersion. The density resolution was estimated around ± 0.001 g/cm^3. The glass samples were weighed in air, (W_{air}), and water (W_{water}), with ($\rho_{water} = 1\,g/cm^3$). Density measurement of each glass samples done using the following relationship:

$$\rho = \frac{W_{air}}{(W_{air} - W_{water})} \quad (1)$$

where (W_{air}) and (W_{water}) each representing the weights of the glass sample in air and distilled water, respectively. Ideally, the glass molar volume is used in describing the network structure and the building units arrangement since it directly deals with the oxygen network spatial structure. Moreover, molar volume (V_m) is considered to be the better tool for studying the changes in glass structure since it eliminates mass from the density and uses an equal number of particles for comparison purposes. It is calculated from density using the equation, ($Vm = M_{glass}/\rho_{glass}$), where ($\rho_{glass}$) is the density of the glass sample and (M_{glass}) is the molecular weight of the glass. The calculation of molar volume for each glass sample was done using the formula:

$$V_m = \frac{\sum_i x_i M_i}{\rho_{glass}} \quad (2)$$

where (M_i) is the oxide component's (i) molecular weight and (x_i) is its mole fraction.

X-ray diffraction (XRD) system PANalytical (Philips) PW3050/60 was used in amorphous nature confirmation in the range of (2θ) value from 4° to 90°. The FTIR spectra were obtained by using the FTIR spectrometer (400–4000 cm^{-1} and resolution of 0.85 cm^{-1} by KBr pellet technique). UV-Vis data was collected using UV-Visible spectrometer (Shimadzu UV-3600-VIS-NIR spectrometer) in the wavelength 200 nm–800 nm.

Results and discussion

Fig. 1 is the glass system's X-ray diffraction pattern. This pattern revealed a broadly diffused scattering around 2θ = 20°–30°. This exhibits the amorphous glass nature and shows the absence of long-range atomic arrangements [12]. Density and calculated values of the molar volume are presented in Table 1 and Fig. 2. Both values were observed to have decreased with increasing amount of ZnO in glass system. The density can be observed to decreased gradually with ZnO percentage. The replacement of ZnO (with lower molecular weight 81.38 g/mol) at the expense of TeO_2 and PbO (with higher molecular weights 159.598 and 223.1994 g/mol, respectively), led to the decrease in density from 6.257 to (6.078 g cm^{-3}) with ZnO content increase from 15 to 25 mol% [13]. Molar volume decreased from 26.22 to 25.40 cm^3/mol with the increasing of ZnO concentration. The glass structure is more explained using molar volume than density, as the former has to do with ions spatial distribution in structure. The molar volume changes with the

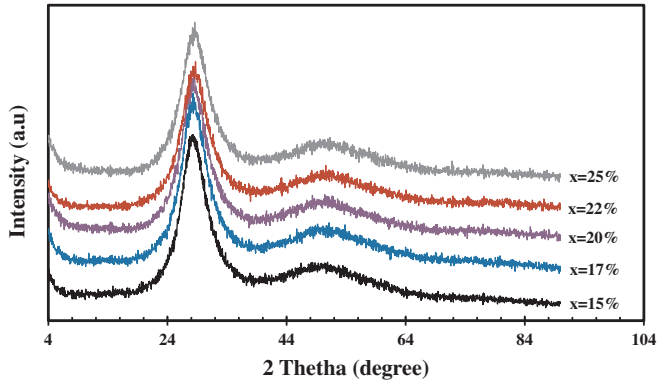

Fig. 1. XRD patterns of $[ZnO]_x$ $[(TeO_2)_{0.7}$-$(PbO)_{0.3}]_{1-x}$glasses.

Table 1
Experimental values of Density (ρ), Molar volume (V_m), Molar refractivity R_m, index and Oxygen packing density (O.P.C) of ternary $[ZnO]_x$ $[(TeO_2)_{0.7}$-$(PbO)_{0.3}]_{1-x}$ glass system.

x (mol%)	ρ (± 32 kg·m^{-3})	V_m (± 0.15 cm^3·mol^{-1})	R_m	(O.P.D)
15	6257	26.22	16.76881143	60.822
17	6230	26.03	17.00987893	60.748
20	6191	25.72	16.39175565	60.568
22	6144	25.60	16.54759886	60.395
25	6078	25.40	16.22142697	60.050

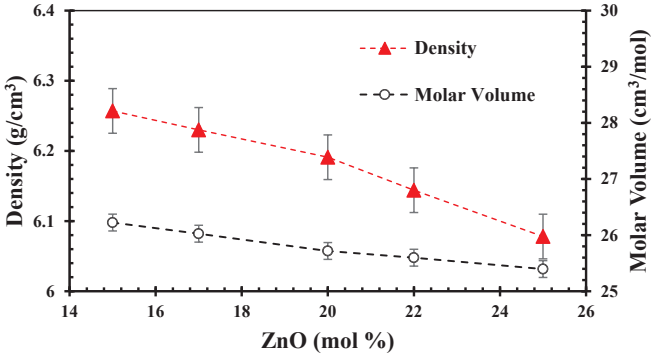

Fig. 2. Density (ρ) and molar volume(V_m) of the $[ZnO]_x$ $[(TeO_2)_{0.7}$-$(PbO)_{0.3}]_{1-x}$glasses.

ZnO molar composition is an indication of the preceding structural changes via a modification or formation process in the network of the glass [14]. Molar volume decreased for the glass system from 26.22 to 25.40 (cm^3/mol) may be due to a bond length reduction or inter-atomic spacing decrease between the constituting atoms in the glasses [15]. Thus, it can be noted that the variation of the densities and molar volume is due to the low change in concentration of ZnO.

The glasses' FTIR spectra in the range 280–4000 cm^{-1}are presented in Fig. 3. The Fig. 3 shows absorption bands with highest intensities around 419 cm^{-1}, and between 596 and 612 cm^{-1}. The vibrations around 419 cm^{-1} is ascribed the stretching vibrations Zn-O in ZnO_4 or of Te-O-Te vibrations or O-Te-O linkages. The absorptions with centers between 596 and 619 maybe attributed to the stretching vibrations of Te-O bonds in the TeO_4 structural units [16]. The shift in the absorption center toward higher wave numbers with increase in the proportion of ZnO might be attributed to the conversion of TeO_4 units to TeO_3 structural units. The TeO_4 to TeO_3 unit conversion indicates the formation of non-bridging oxygens [17]. Between 664 and 677 cm^{-1}, the IR absorption maybe either due to Te-O vibrations in TeO_3 structural

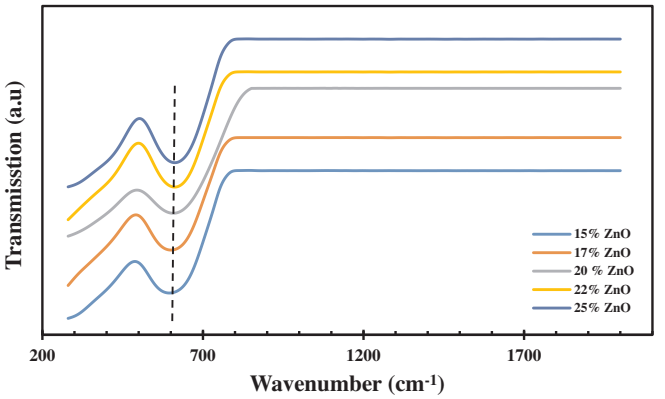

Fig. 3. FTIR spectra of $[ZnO]_x$ $[(TeO_2)_{0.7}$-$(PbO)_{0.3}]_{1-x}$glasses with x = 0.15, 0.17, 0.20, 0.22, 0.25 mol%.

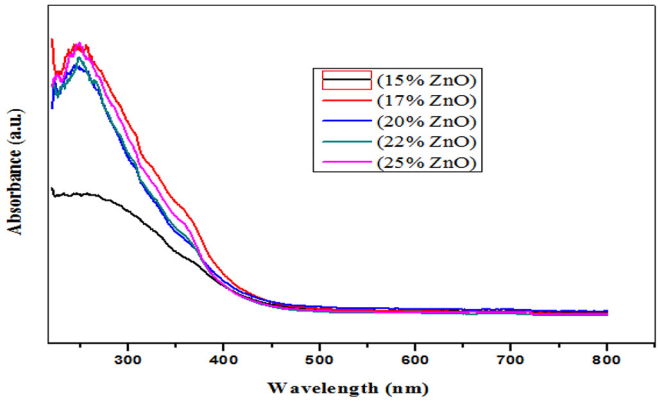

Fig. 4. UV absorption spectra of $[ZnO]_x$ $[(TeO_2)_{0.7}$-$(PbO)_{0.3}]_{1-x}$ glasses with x = 0.15, 0.17, 0.20, 0.22, 0.25 mol%.

units or the vibrations of Pb-O in PbO_3 or PbO_4 structural units [17].

The determination of both optical band gaps (Direct and Indirect) was carried out using the expression of Davis and Mott [18] for the coefficient of absorption α (υ) as;

$$\alpha(\upsilon) = B\frac{(h\upsilon - E_{opt})^n}{h\upsilon} \tag{3}$$

where E_{opt} representing the optical band gap, n is a number, with indirect and direct allowed transitions are denoting $n = 2$ and $n = 1/2$ and B = constant. This absorption coefficient value $\alpha(\upsilon)$ is the determined by the expression, with A obtained from the UV-Vis spectra in Fig. 4;

$$\alpha(\upsilon) = 2.303\frac{A}{t} \tag{4}$$

where t = sample thickness, A = optical absorbance value. By drawing the Tauc's plots between $(\alpha\hbar\omega)^{1/n}$ and the photon energy $(\hbar\omega)$ and extrapolating the linear part of the plots, optical band gap values where obtained at$(\alpha\hbar\omega)^{1/2} = 0$ and $(\alpha\hbar\omega)^2 = 0$ respectively for the indirect and direct transitions [19,20]. The optical band gap values both direct and indirect were presented in as shown in Figs. 5, 6 and Table 2. The direct and indirect varied between 3.41 and 3.89 eV and 2.40 and 2.63 eV due to the ZnO content is increased from 0.15 to 0.17, 0.20, 0.22 and 0.25 mol% respectively. In both cases, the values increase with the increasing concentration of Zn^{2+} ions may be to the bridging of the free space in the glass. This results to an increase in the structural compactness in the network of the glass [21]. The decrease in the values of both band gaps (indirect and direct) may be attributed to the electron localization degree that is caused by the glass network's structural changes. The coefficient of absorption, $\alpha(\upsilon)$ of the glasses is expressed

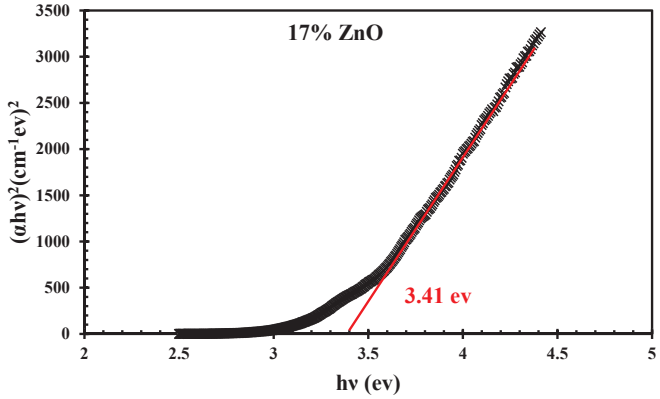

Fig. 5. The optical band gap of $[ZnO]_x$ $[(TeO_2)_{0.7}$-$(PbO)_{0.3}]_{1-x}$ glasses, x = 0.17 mol%.

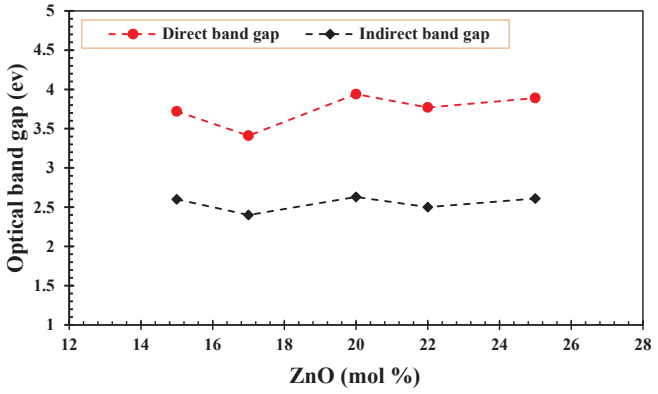

Fig. 6. Energy gap values for $[ZnO]_x$ $[(TeO_2)_{0.7}$-$(PbO)_{0.3}]_{1-x}$glasses with x = 0.15, 0.17, 0.20, 0.22, 0.25 mol%.

as the photon energy $(h\upsilon)$ exponential function and B as a constant value [22];

$$\alpha(\upsilon) = B\ exp\frac{h\upsilon}{\Delta E} \tag{5}$$

The values of the Urbach energy as observed in Table 2 varies with the concentration of Zn^{2+} ions in the network from 0.15 to 0.17, 0.20, 0.22 and 0.25 mol%. The Urbach energy decrease shows an increase in the glass fragility due to increase in the TeO_3 concentration that changes the structural networking in the glass. This indicates defects formation and hence causes the band gap value increase, whereas the increase is an indication of defects deformation and results from an increase in the BOs number.

Figs. 7 and 8 present the index of refraction (n) and the oxygen packing density respectively. The refractive index (n) of the prepared glass system was calculated values of the optical energy band gap (Indirect, E_{indir}) using the equation in [22].

$$\frac{n^2-1}{n^2+2} = 1-\sqrt{\frac{E_{opt}}{20}} \tag{6}$$

The refractive index as presented in Fig. 7 varies with ZnO concentration from 0.15 to 0.25 in the glass system. The increase may be associated with the substitution of TeO^{4+} and $Pb^{2+}$with Zn^{2+} ions with lower polarizability [23]. Whereas the decrease in the refractive index may be associated with the decrease in the NBOs concentration in the glass network [24]. The oxygen packing density in Fig. 8 and Table 1 decreased with ZnO concentration increased. This showed a same relation with the molar volume as presented in Fig. 1 and Table 1. The decrease indicates a more spatial distribution of oxygen in the glass network. This can be associated with a Te^{4+} substitution and Pb^{2+} with higher field intensity than Zn^{2+} hence, having a lower attraction to the oxygen atoms [25].

For any material, the metallization criterion gives information about the metallic or insulating nature of such material on its band gap energy basis and is expressed as a function of molar refraction (R_m) and molar volume (V_m) as reported by [26] as;

$$M = 1-\frac{R_m}{V_m} \tag{7}$$

The molar polarizability, transmission coefficient, reflection loss, dielectric constant, optical dielectric constant and oxide ion polarizability were calculated using Eqs. (8)–(13) respectively.

$$\alpha_m = \left(\frac{3}{4\pi N}\right)R_m \tag{8}$$

$$R_L = \left[\frac{n-1}{n+1}\right]^2 \tag{9}$$

Table 2
Direct and Indirect band gap, Urbach energy, Refractive index, Molar refraction and Reflection loss.

x (mol%)	Direct band gap (± 0.092 eV)	Indirect band gap (± 0.043 eV)	Urbach energy (± 0.018 eV)	Refractive index, n (± 0.146)	Molar refraction, R_m (± 0.14) cm^3)	Reflection Loss, R_L
15	3.72	2.6	0.354	2.51	16.76	0.185
17	3.41	2.40	0.2764	2.58	17.00	0.194
20	3.94	2.63	0.3323	2.50	16.39	0.184
22	3.77	2.50	0.2624	2.54	16.54	0.190
25	3.89	2.61	0.2724	2.51	16.22	0.185

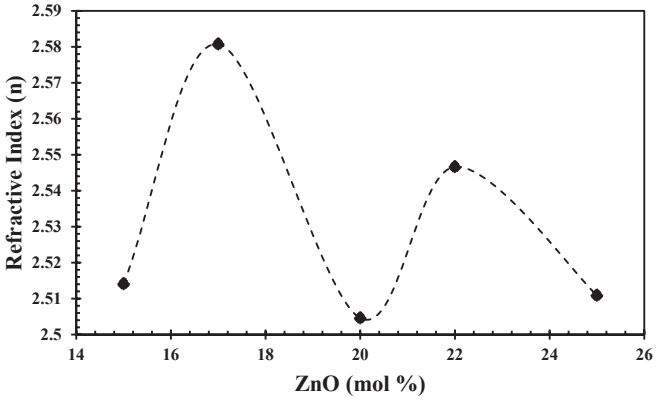

Fig. 7. Refractive index of $[ZnO]_x$ $[(TeO_2)_{0.7}$-$(PbO)_{0.3}]_{1-x}$glasses with x = 0.15, 0.17, 0.20, 0.22, 0.25 mol%.

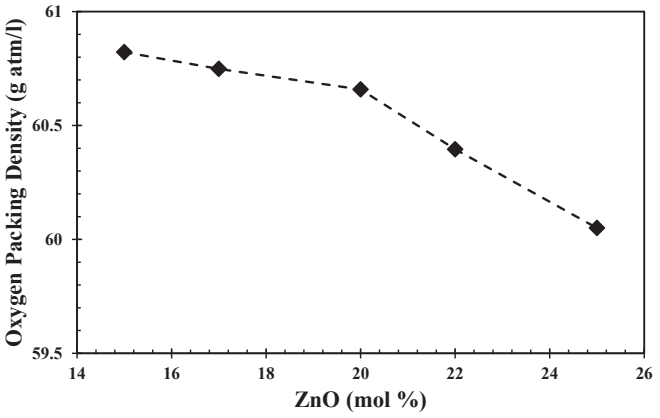

Fig. 8. Oxygen packing density of$[ZnO]_x$ $[(TeO_2)_{0.7}$-$(PbO)_{0.3}]_{1-x}$, x = 0.15, 0.17, 0.20, 0.22,0.25 mol%.

$$T = \frac{2n}{n^2 + 1} \tag{10}$$

The dielectric constant is inversely proportional to the square of the speed of light in the material [27],

$$\varepsilon = n^2 \tag{11}$$

$$\varepsilon_{opt} = p\frac{dt}{dp} = \varepsilon - 1 = n^2 - 1 \tag{12}$$

The oxide ion polarizability based on refractive index was calculated as reported by Meena and Bhatia [9].

$$\alpha_{O^{2-}}^{(n)} = \left[\frac{R_m}{2.52} - \sum \alpha_i\right] \left(N_{O^{2-}}\right)^{-1} \tag{13}$$

where $\Sigma\alpha_i$ = molar cation polarizability and $N_{O^{2-}}$ is the oxide ions number in the chemical formula. The values of the molar cation polarizability (α) was obtained as reported in [28]. In Table 3, the metallization criterion, molar polarizability, transmission coefficient, dielectric constant and oxide ion polarizability were presented. Decrease

Table 3
Metallization Criterion, Molar Polarizability, Optical Transmission Coefficient, Dielectric Constant and Oxide Ion Polarizability.

x (mol%)	M	α_m	α_e	T	ε	ε_{opt}	$\alpha_{\bar{O}2}(n)$
15	0.360	6.65	0.2535	0.686	6.32	5.3205	1.579
17	0.346	6.74	0.2591	0.673	6.66	5.6602	1.624
20	0.362	6.50	0.2526	0.688	6.27	5.2729	1.561
22	0.353	6.56	0.2562	0.680	6.48	5.4853	1.595
25	0.361	6.43	0.2532	0.687	6.30	5.3045	1.571

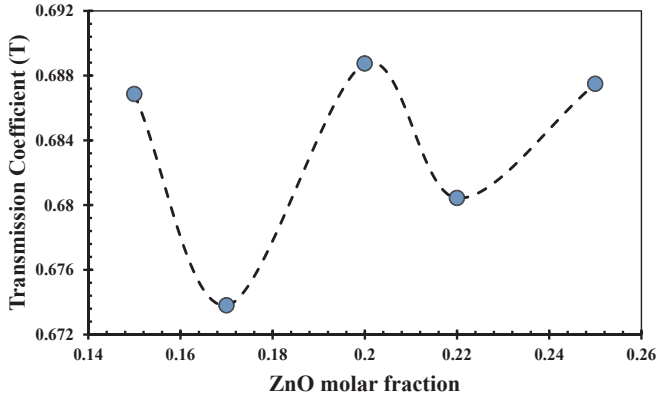

Fig. 9. Optical Transmission Coefficient of $[ZnO]_x$ $[(TeO_2)_{0.7}$-$(PbO)_{0.3}]_{1-x}$, x = 0.15, 0.17, 0.20, 0.22,0.25 mol%.

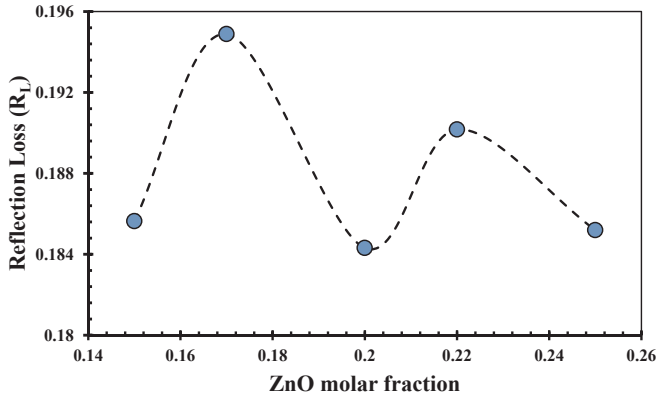

Fig. 10. Reflection Loss of $[ZnO]_x$ $[(TeO_2)_{0.7}$-$(PbO)_{0.3}]_{1-x}$, x = 0.15, 0.17, 0.20, 0.22,0.25 mol%.

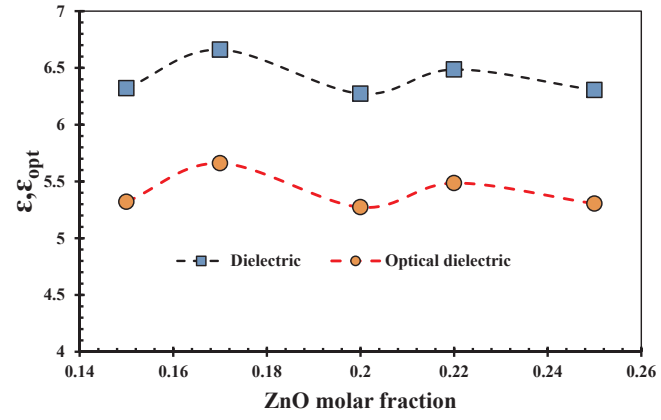

Fig. 11. Dielectric and Optical Dielectric Constants of $[ZnO]_x$ $[(TeO_2)_{0.7}$-$(PbO)_{0.3}]_{1-x}$, x = 0.15, 0.17, 0.20, 0.22,0.25 mol%.

in the value of metallization criterion is an indication that the width of both the conduction and valence band has increased with the addition of more ZnO in the network [7]. The dielectric constant values in any glass system depend on their ionic polarizability, electronic polarizability, and the contribution of dipole orientation to the polarizability. The observed behavior of the dielectric constant as shown in Fig. 11 in the studied glasses may be associated to low frequency in the polarization caused by multi-component contributions in the system of the studied glasses [29]. Because of its dependence on the molar volume and refractive index, the polarizability value increased in the glasses with an increase in the ZnO content may be associated with the increase

Table 4
Number of bond per unit volume (n_b), polaron radius (R_p), Inter-nuclear distance of Zn^{2+} (R_i), Field Strength of Zn^{2+} yield, molar volume of tellurium atoms (V_{Te}) and average Te to Te separation ($\langle d_{Te\text{-}Te}\rangle$).

x (mol%)	n_b	R_p (Å)	R_i (Å)	F (cm^{-2})	V_{Te}	$\langle d_{Te\text{-}Te}\rangle$
15	9.185E+22	2.6689	6.6222	11.512	32.375	3.775E−08
17	9.255E+22	2.5533	6.3355	12.578	31.056	3.723E−08
20	9.366E+22	2.4091	5.9777	14.129	29.225	3.648E−08
22	9.410E+22	2.3302	5.7818	15.102	28.191	3.605E−08
25	9.485E+22	2.2270	5.5260	16.533	26.732	3.541E−08

in the molar volume increased in the glass network. Whereas the decrease in the values may be connected to the substitution of higher polarizability Te^{4+} and Pb^{2+} ions with lower polarizability Zn^{2+} ions in the glass network and also decrease in the inter-ionic distances [30–32].

The parameters presented in Table 4 were obtained as reported by [33] as follows; Average Tellurium-Tellurium separation, $\langle d_{Te\text{-}Te}\rangle$;

$$\langle d_{Te-Te}\rangle = \left[\frac{V_m^{Te}}{N_A}\right]^{1/3} \tag{14}$$

$$\text{Where } V_m^{Te} = \frac{V_m}{2(1-X_{Te})} \tag{15}$$

Zn^{2+} ion concentration, N is expressed as;

$$N\,(Zn^2) = \frac{X_{Zn}x\rho xN_A}{m_w} \tag{16}$$

where N_A, V_m^{Te}, X_{Te} and X_{Zn} are the Avogadro's number, molar volume of tellurium atoms, molar fraction of tellurium and molar fraction of zinc respectively. The average Te-Te separation helps in explaining the changes in glass material compactness and rigidity and thus, can be used to explain the changes in optical band gap [34].

Polaron radius (R_p), inter-ionic distance of Zn^{2+} ions (R_i) and field strength of Zn^{2+} yield (F) for the glasses was obtained using the equation as reported [33,35] as;

$$R_p = \frac{1}{2}\left(\frac{\pi}{6N}\right)^{1/3} \tag{17}$$

$$R_i = \left(\frac{1}{N}\right)^{1/3} \tag{18}$$

$$F = \frac{Z}{r_p^2} \tag{19}$$

In Fig. 12 and Table 4 below, the polaron radius value of the ZnO-PbO-TeO_2 glass system studied decreased from 2.6689 to 2.2270 Å when the concentration of Zn^{2+} was increased from 15% to 25%. This

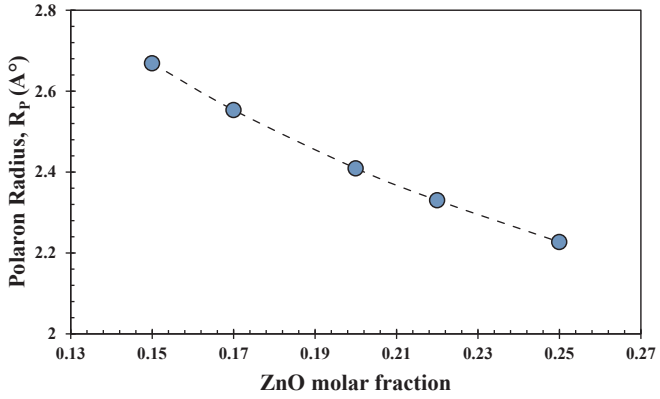

Fig. 12. Polaron Radius of $[ZnO]_x$ $[(TeO_2)_{0.7}$-$(PbO)_{0.3}]_{1-x}$, x = 0.15, 0.17, 0.20, 0.22, 0.25 mol%.

may be due to an increase in polarizability and material compactness in the glass [33]. Polaron radius decrease may eventually lead to an increase in the glass electrical conductivity [36]. The average Te to Te ion distance in the glass system as presented in Table 4 continued to decrease as the amount of Zn^{2+} ions are increased in the system. Figs. 9 and 10 present the variations of transmission coefficient and reflection loss with Zn^{2+} ions concentrations. The values showed an inverse relation between the two parameters which agrees with the theoretical submission that the transmission increases when reflection decreases and vice versa [37]. The 17% ZnO composition provides the best ZnO proportion for optical and fiber applications due to its refractive index [33]. Average coordination number (m) and number of bond per unit volume where calculated using the next equations respectively as reported previously [33].

$$m = \sum_i n_{ci} x_i \tag{20}$$

$$N_b = \frac{N_A}{V_m} m \tag{21}$$

where Z is the atomic number of erbium, n_{ci} is the coordination number of the cations and x_i is molar concentration of the cations. The glass system's coordination number m remained at a value 4.0 for all the ZnO concentrations studied, while the number of bonds per unit volume increased from 9.185×10^{22} to $9.485 \times 10^{22}\,cm^{-3}$. This is an indication of increase in the glass rigidity, material compactness, glass transition temperature and elastic modulus of the glasses [38,39].

Conclusion

New tellurite glasses with chemical composition $[ZnO]_x\,[(TeO_2)_{0.7}\text{-}(PbO)_{0.3}]_{1\text{-}x}$, where x = 0, 0.15, 0.17, 0.20, 0.22 and 0.25 mol% have been achieved. XRD analysis was carried out to confirm the amorphous nature of the glasses. FTIR analysis from 280 to 4000 cm^{-1} revealed the presence of TeO_4 and TeO_3 units in the glasses. The values of the direct, indirect band gap ranged from 3.41 to 3.94 eV and 2.40 to 2.63 eV respectively as ZnO increased from 15 to 25 mol%.

Also, refractive index changed from 2.5 to 2.58 (± 0.146), metallization criterion 0.346–0.361, oxide ion polarizability 1.561–1.561, average tellurium-tellurium distance 3.541E − 08 to 3.775E − 08 and polaron radius 2.6689–2.2270 (Å). Reflection loss and the dielectric constants changed in a reversed manner to the band gap and Urbach energy.

Acknowledgements

The researchers acknowledged with gratitude the financial support for this work by the Malaysian Ministry of Higher Education (MOHE) and Universiti Putra Malaysia through the Fundamental Research Grant Scheme (FRGS) and Inisiatif Putra Berkumpulan (IPB) research grant. The authors would like to also acknowledge the contributions of the reviewers of this paper toward ensuring quality in both presentation and substance.

References

[1] Uma V, Vijayakumar M, Marimuthu K, Muralidharan G. Luminescence and energy transfer studies on Sm^{3+} /Tb^{3+} codoped telluroborate glasses for WLED applications. J Mol Struct 2018;1151:266–76.
[2] El-Mallawany R, Sayyed MI, Dong MG. Comparative shielding properties of some tellurite glasses: part 2. J Non-Crystalline solids 2017;474:16–23.
[3] Abdel-Kader A, El-Mallawany R, Elkholy MM. Network structure of tellurite phosphate glasses: optical absorption and infrared spectra. J Appl Phys 1993;73:71–4.
[4] Moawad HMM, Jain H, El-Mallawany R, Ramadan T, El-Sharbiny M. Electrical conductivity of silver vanadium tellurite glasses. J Am Ceram Soc 2002;85:2655–9.
[5] Hager IZ, El-Mallawany R, Bulou A. Luminescence spectra and optical properties of TeO_2–WO_3–Li_2O glasses doped with Nd, Sm and Er rare earth ions, Physica B: Condensed Matter 406 (2011), 972–980. Idem, ibid 2011;406:1844.
[6] Taylor P, Trioxide C, Nanoplatlets G, Gautam C, Dixit S, Madheshiya A. Spectroscopy letters : an international journal for synthesis and structural properties of lead strontium titanate borosilicate glasses with addition of synthesis and structural properties of lead strontium titanate borosilicate glasses with addition of C. An Int J Rapid Commun 2014;48(4):280–5.
[7] Kaky KM, Lakshminarayana G, Baki SO, Kityk IV, Taufiq-yap YH, Mahdi MA. Results in physics structural, thermal and optical absorption features of heavy metal oxides doped tellurite rich glasses. Results Phys 2017;7:166–74.
[8] Marzouk SY, Gaafar MS. Ultrasonic study on some borosilicate glasses doped with different transition metal oxides. Solid State Commun 2007;144:478–83.
[9] Meena SL, Bhatia B. Polarizability and optical basicity of Er 3+ ions doped zinc lithium bismuth borate glasses. J. Pure Appl. Ind. Phys. 2016;6(10):175–83.
[10] Thirumaran S, Sathish K. Spectroscopic investigations on structural characterization of borate glass specimen doped with transition metal ions. Res J Chem Environ 2015;18(10):77–82.
[11] Matori KA, Hafiz M, Zaid M, Quah HJ, Hj S, Aziz A, et al. Studying the effect of ZnO on physical and elastic properties of (ZnO) x (P 2 O 5) 1 − x glasses using non-destructive ultrasonic method. Adv Mater Sci Eng 2015;2015:6.
[12] El-Zaidia MM, Ammar AA, El-Mallwany RA. Infra-red spectra, electron spin resonance spectra, and density of $(TeO_2)_{100-x}-(WO_3)_x$ and $(TeO_2)_{100-x}-(ZnCl_2)_x$ glasses. Phys Status Solidi (a) 1985;91(2):637–42.
[13] Sidek HAA, El-Mallawany R, Siti SB, Halimah MK, Khamirul AM. Optical properties of erbium zinc tellurite glass system. Adv Mater Sci Eng 2015;628954. http://dx.doi.org/10.1155/2015/628954.
[14] Hafiz M, Zaid M, Matori KA, Aziz SHA, Zakaria A, Sabri M, et al. Effect of ZnO on the physical properties and optical band gap of soda lime silicate glass. Int. J. Mol. Sci Int. J. Mol. Sci 2012;13:7550–8.
[15] Azuraida A, Halimah MK, Sidek AA, Azurahanim CAC, Iskandar SM, Ishak M, Nurazlin A. Comparative studies of bismuth and barium boro-tellurite glass system: structural and optical properties. Chalcogenide Lett 2015;12(10):497–503.
[16] Mansour E. FTIR spectra of pseudo-binary sodium borate glasses containing TeO 2. J Mol Struct 2012;1014:1–6.
[17] Rada S, Dehelean A, Culea E. FTIR and UV-VIS spectroscopy investigations on the structure of the europium-lead-tellurate glasses. J Non-Cryst Solids 2011;357(16–17):3070–3.
[18] Mott NF, Davies EA. Electronic Processes in Non-Crystalline Materials. Oxford: Clarendon Press; 1979.
[19] Escobar-Alarcón L, Arrieta A, Camps E, Muhl S, Rodil S, Vigueras-Santiago E. An alternative procedure for the determination of the optical band gap and thickness of amorphous carbon nitride thin films. Appl. Surf. Sci. 2007;254(1 Spec. Iss.):412–5.
[20] Said Mahraz ZA, Sahar MR, Ghoshal SK, Ashur Z, Mahraz S, Sahar MR, Ghoshal SK. Band gap and polarizability of boro-tellurite glass: Influence of erbium ions. J Mol Struct J 2014;1072(1):238–41.
[21] Thakur V, Singh A, Punia R, Dahiya S, Singh L. Structural properties and electrical transport characteristics of modified lithium borate glass ceramics. J Alloys Compd 2017;696:529–37.
[22] El-Mallawany R, Abdalla MD, Ahmed IA. New tellurite glass: optical properties. Mater Chem Phys 2008;109(2–3):291–6.
[23] Linda D, Duclère J-R, Hayakawa T, Dutreilh-Colas M, Cardinal T, Mirgorodsky A, Kabadou A, Thomas P. Optical properties of tellurite glasses elaborated within the TeO_2 –Tl_2O-Ag_2 O and TeO_2 –ZnO–Ag_2O ternary systems. J Alloys Compd 2013;561:151–60.
[24] Azlan MN, Halimah MK, Sidek HAA. Linear and nonlinear optical properties of erbium doped zinc borotellurite glass system. J Lumin 2017;181:400–6.
[25] Rao VH, Prasad PS, Rao PV, Santos LF, Veeraiah N. Influence of Sb 2 O 3 on tellurite based glasses for photonic applications. J Alloys Compd 2016;687:898–905.
[26] Berwal N, Dhankhar S, Sharma P, Kundu RS, Punia R, Kishore N. Physical, structural and optical characterization of silicate modified bismuth-borate-tellurite glasses. J Mol Struct 2017;1127:636–44.
[27] Ramadevudu G, Chary MN. Physical and spectroscopic studies of Cr 3 þ doped mixed alkaline earth oxide borate glasses. Mater Chem Phys 2017;186:382–9.
[28] Umar SA, Halimah MK, Chan KT, Latif AA. Polarizability, optical basicity and electric susceptibility of Er 3 + doped silicate borotellurite glasses. J Non Cryst Solids 2017;471(March):101–9.
[29] Thombre DB. The Estimation of Oxide Polarizability using the Electronegativity for Li_2O : B_2O_3: SiO_2 Glass System. Int J Sci Eng Technol 2014;3(8):1047–50.
[30] Guo H, Wang Y, Gong Y, Yin H, Mo Z, Tang Y, Chi L. "Optical band gap and photoluminescence in heavily Tb 3 þ doped GeO2-B2O3-SiO2-Ga2O3 magneto-optical glasses," 2016'686:635–40.
[31] Selvi S, Marimuthu K, Murthy NS, Muralidharan G. Red light generation through the lead boro À telluro À phosphate glasses activated by Eu 3 þ ions. J Mol Struct 2016;1119:276–85.
[32] Pawar PP, Munishwar SR, Gedam RS. Intense white light luminescent Dy 3 þ doped lithium borate glasses for W-LED : A correlation between physical, thermal, structural and optical properties. Solid State Sci 2017;64:41–50.
[33] Umar SA, Halimah MK, Chan KT, Latif AA., "Physical, structural and optical properties of erbium doped rice husk silicate borotellurite (Er-doped RHSBT) glasses," J Non Cryst Solids, 2017;no. July:0–1.
[34] Annapoorani K, Murthy NS, Ravindran TR, Marimuthu K. Influence of Er 3+ ion concentration on spectroscopic properties and luminescence behavior in Er 3+ doped Strontium telluroborate glasses. J Lumin 2016;171:19–26.
[35] Byrnes SJF. "Basic theory and phenomenology of polarons," 2008:2–6.
[36] Landau LD, Pekar SI. Effective mass of a polaron. Zh Eksp Teor Fiz 1948;18(5):71–4.
[37] Bounakhla M, Tahri M. "X-ray fluorescence analytical techniques," Rabat, Morocco, 2014.
[38] Ersundu MC, Ersundu AE. Structure and crystallization kinetics of lithium tellurite glasses. J Non Cryst Solids 2016;453:150–7.
[39] El-Mallawany R. Tellurite glasses Part 1. Elastic properties. Mater Chem Phys 1998;53:93–120.